ACS APPLIED POLYMER MATERIALS

pubs.acs.org/acsapm

Article

Collagen-Based Micro/Nano Fibrous Constructs: Step-By-Step Reverse Biomimetics of Structure and Mechanical Function

Smadar E. Sharon, Adi Aharonov, Haim S. Mordechai, Javad Tavakoli, and Mirit Sharabi*

Cite This: *ACS Appl. Polym. Mater.* 2023, 5, 2816−2829

Read Online

ACCESS | Metrics & More | Article Recommendations

ABSTRACT: Multiscale micro−nano fibrous structures are a cutting-edge research area in material science and have drawn the attention of scientists in recent years. These structures are widely distributed in nature's materials and hold fascinating and unique properties, such as mechanical behaviors, high surface area to volume ratio, and special multiscale biological functionalities. Herein, we demonstrate step-by-step biomimetics of a multiscale composite material system and the influence of the different structural mechanisms on mechanical behavior. This is done using systematic biomimetics and investigation of the mechanical effect of every constituent. We have fabricated and characterized mechanically and structurally different material systems to get a comprehensive understanding of the structure−function relationship in multiscale biomimetic constructs (MSBCs) and examine the influence of the material selection and structure. We first characterized the electrospun nanofibers made of polyamide 6 (PA6) and gelatin-polyamide 6 (GPA6) and then constructed and characterized the combined constructs. Our micro−nano fibrous structures were constructed from combined unique coral collagen microfibers and PA6 and GPA6 nanofibers. These hierarchical structures demonstrated an entangled network of nanobridges among the micro collagen fibers. However, the GPA6-collagen structures showed better connectivity with the microfibers and were significantly stiffer and stronger than the PA6-collagen structures due to the material compatibility. Furthermore, our structures demonstrated a considerable resemblance with soft tissue structures. We embedded the MSBC in alginate hydrogel to form biocomposites that displayed a hyperelastic nonlinear behavior with significantly improved toughness and a remarkable similarity to the mechanical behavior of native soft tissues. Our results present great potential to be further developed as tailor-designed multiscale next-generation specialized structures for soft tissue repair and replacement.

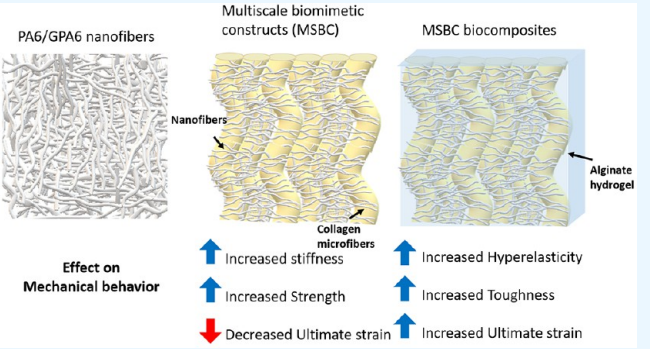

KEYWORDS: *micro−nano, mechanical behavior, multiscale, electrospinning, fibrous materials, structural materials, collagen*

1. INTRODUCTION

Through billions of years of evolution, soft tissues developed highly intricate and efficient fibrous network structures, resulting in enhanced mechanical properties and structural complexity alongside remarkable biological activity.[1−6] These composite fibrous networks, the extracellular matrix (ECM), are organized in a multiscale hierarchy from the nano to the macro scale, creating a complex hierarchical structure of fibrils and fibers. Bridging the multiscale gap between multiscale structures and their roles in the tissues' mechanical properties is essential for creating soft tissue biomimetic analogues together with next-generation material systems.[7] The unique mechanical behavior of soft tissues (such as large deformations, viscoelasticity, and strain stiffening) is crucial for their everyday function. A proper soft tissue analogue should be mechanically biocompatible with the native tissue, since a mismatch in the mechanical behavior can result in stress concentration, hyperplasia, and failure, together with additional short and long-term health impairments.[8] Therefore, mimicking the structural complexity manifested in different structural mechanisms (such as fiber crimping, multiscale arrangement, weak interactions that allow inner sliding, etc.)[9] enables the mimicry of complex soft tissue mechanics.

From a mechanical point of view, all of these soft tissues largely consist of similar materials: collagen, elastin, and proteoglycans (PGs).[10] Type I collagen is the main structural protein in the ECM and provides strength and stiffness.[11−13] The soluble PGs dissolve and diffuse freely in the interfibrillar space and increase the total volume of the fiber network, forming

Received: January 9, 2023
Accepted: March 20, 2023
Published: March 29, 2023

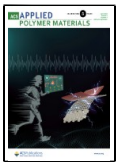

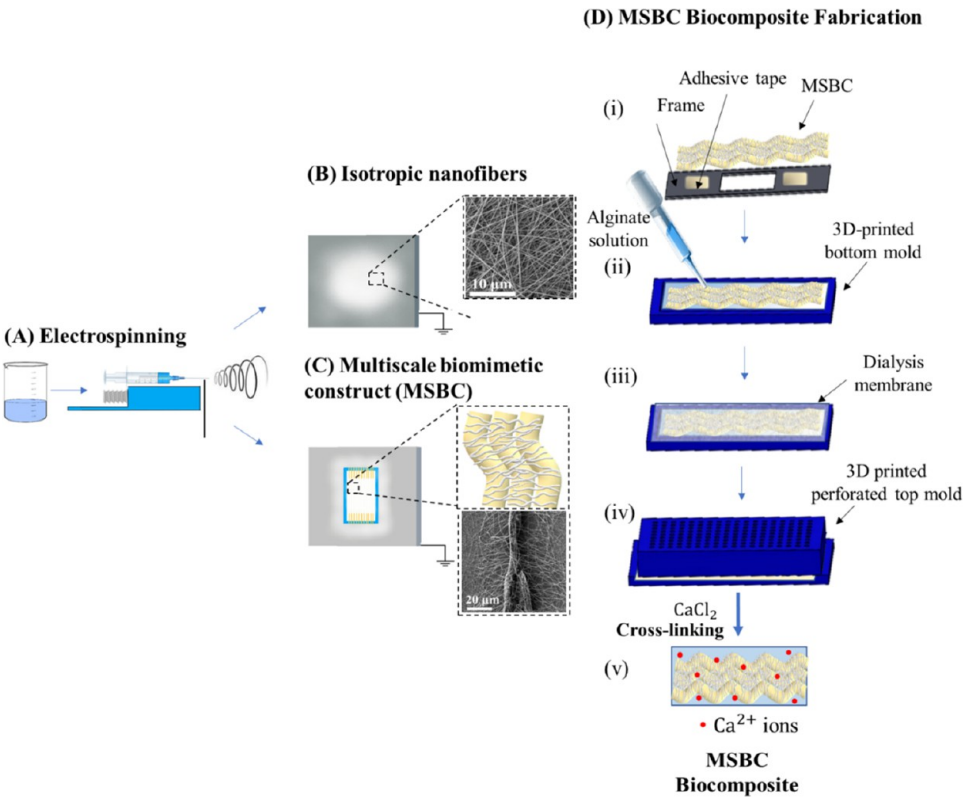

Figure 1. Illustration of the fabrication process. (A) Electrospinning of PA6 and GPA6. (B) Fabrication of the isotropic nanofibers by a static collector. (C) Fabrication of multiscale biomimetic constructs (MSBCs). (D) Fabrication of MSBC biocomposite. (i) MSBC samples were glued to a 3D-printed frame. (ii) MSBC samples with frames were inserted into a 3D-printed bottom mold and covered with an alginate solution. (iii) Bottom mold with the MSBC and alginate was covered with a dialysis membrane. (iv) 3D-printed perforated top mold was located on the bottom mold to close it. (v) Closed mold was inserted into $CaCl_2$ solution to cross-link the alginate and create the biocomposite.

aqueous surroundings and shock absorbance ability.[14] Elastin provides flexibility and fatigue endurance.[9,15−19] The configuration and arrangement of these networks govern the form and function of the tissue,[20] and they have a crucial fundamental role in preventing premature failure in tissues.[9,13]

Furthermore, fibrous networks also allow energy transmission, storage, and dispersion, providing soft tissues with effective locomotion, movement, and regeneration abilities. It is amazing that diverse and multiple functions and properties can be derived from this set of three materials. Biomimetics of these multiscale nano-to-micro fibrous structures is a cutting-edge research area in the field of materials science, with immense influence on tissue engineering research and additional areas such as drug delivery, wound healing, and biosensing.[21]

Fabrication of the multiscale structures has been produced from natural and synthetic polymers to create different geometries, such as fibers, spheres, and particles.[21] Different techniques, such as phase separation,[22] freeze-drying,[23] 3D printing,[24,25] microfluidic spinning,[26] and electrospinning,[27−32] were employed toward that goal.[29−32] These 3D multiscale structures resemble fibrous networks in natural materials (i.e., soft tissues) with high porosity and enhanced biological properties.[33−35] However, the mechanical behavior of these multiscale micro-to-nano structures and their contribution to the structure−function relationships are yet to reveal.

Our previous studies demonstrated the fabrication of hierarchical biocomposites[36] and the use of coral collagen fibers reinforced biocomposites with similar mechanical and biological properties compared to soft tissues.[37−42] Here, inspired by the fibrous networks in natural materials, we developed a universal method for the simple fabrication of biomimetic constructs that resemble the structure of soft tissues at multiscale ranges (from nano to micro scales) toward mimicking their structure−function relationship[43] in a complex composite construct. We fabricated the composites step by step to get an understanding of the isolated mechanical contribution of the different constituents. We combined natural coral collagen microfibers with polyamide and gelatin electrospun nanofibers to create multiscale biomimetic constructs (MSBCs) and characterized their structure and mechanical function. Then, these MSBCs were embedded in an alginate hydrogel to provide aqueous surroundings to create biocomposites. Structural and mechanical characterizations were done to identify the impact of the multiscale arrangement of fibers on the structure−function relationships of the constructs.

2. MATERIALS AND METHODS

2.1. Polyamide 6 (PA6) and Gelatin-Polyamide 6 (GPA6) Solution Preparation. Polycaprolactam (polyamide 6) pellets (181110, Sigma-Aldrich, Israel) were dissolved in formic acid (F0507, Sigma-Aldrich, Israel) and acetic acid (A6283, Sigma-Aldrich, Israel) in a 2:1 weight ratio, respectively, to prepare polyamide 6 (PA6) solution (12.6 wt %). Gelatin-polyamide 6 (GPA6) solution (18 wt %) was prepared from PA6 pellets and commercial gelatin powder in a 70:30 weight ratio, respectively. The polymers were dissolved in formic acid and acetic acid in the same weight ratio (2:1). The solutions were produced at room temperature under constant stirring for 24 h. Coral collagen fibers were extracted from soft coral Sarcophyton sp. colonies that were frozen and thawed before fiber extraction as previously described.[40−42]

https://doi.org/10.1021/acsapm.3c00057
ACS Appl. Polym. Mater. 2023, 5, 2816−2829

Table 1. Geometry of the Tested Samples

samples	n	thickness (μm)	width (mm)	length (mm)	FVF (%)	UTS (MPa)	strain at UTS (mm/mm)
GPA6 isotropic nanofibers networks	6	105.2 ± 6.6	5.9 ± 0.4	10.0 ± 1.0		4.0 ± 0.6	0.31 ± 0.06
PA6 isotropic nanofibers networks	5	75.2 ± 19.0	5.9 ± 0.4	7.4 ± 0.5		2.8 ± 0.2	0.17 ± 0.00
collagen-GPA6 MSBC	7	107.1 ± 14.6	5.9 ± 0.4	9.0 ± 0.3	15	9.0 ± 1.9	0.22 ± 0.02
collagen-PA6 MSBC	9	132.3 ± 23.7	4.9 ± 0.4	7.8 ± 1.0	12	6.2 ± 1.6	0.24 ± 0.04
collagen-GPA6 MSBC biocomposites	5	339.6 ± 86.5	5.3 ± 0.1	8.6 ± 0.6	26	3.3 ± 1.0	0.36 ± 0.02
collagen-alginate biocomposites (0.2)	12	491.6 ± 126.8	7.6 ± 0.5	16.8 ± 1.5	20	1.3 ± 0.6	0.20 ± 0.03
collagen-alginate biocomposites (0.3)	4	300.4 ± 61.6	7.9 ± 0.3	17.4 ± 1.2	30	2.1 ± 0.6	0.16 ± 0.02

2.2. Electrospinning of PA6 and GPA6. The electrospinning apparatus consisted of a high-voltage power supply (ES30R-5W, Gamma High Voltage Research Inc.), a syringe pump (NE-300, New Era Pump Systems Inc.), and a static collector (Figure 1B,C). The collector was covered with aluminum foil and grounded. The solution was loaded with a 1 mL plastic syringe with a 20G needle with a flow rate of 0.4 mL/h. The distance between the needle tip and the collector was 12 cm, and the applied voltage was 22 kV. The electrospinning time was varied according to the preferred thickness, and the environmental conditions were monitored using a humidity and temperature sensor.

2.3. Fabrication of Multiscale Biomimetic Constructs (MSBCs). Soft coral Sarcophyton sp. colonies were kept frozen and thawed before fiber extraction. Pieces of coral were harvested, and the collagen fibers were exposed by reaping the edge of the coral, as previously described.[37,41,42,44,45] The extracted collagen fibers were then wrapped around a thin rectangular metal frame (70×30 mm^2) to create parallel, organized fiber arrays. The microfibers were aligned unidirectionally (0°). The collagen microfibers were washed with double-distilled water (DDW) and dehydrated through a series of graded ethanol solutions. To create the nanofibers on top of the microfibers, we used electrospinning of GPA6/PA6 (Figure 1C). The frame with aligned collagen microfibers was grounded and attached to the static collector. 0.5 mL of PA6 or GPA6 solution was electrospun on every side of the frame to create the multiscale structure. The electrospun nanofiber mats were fabricated directly on top of the collagen microfibers and fully covered on both sides.

2.4. Fabrication of Collagen-Alginate Biocomposites and MSBC Biocomposites. MSBC biocomposites were fabricated using the GPA6 MSBC samples described in Section 2.3. GPA6 MSBC samples were cut and peeled from the aluminum foil and metal frame. They were glued to 3D-printed frames ($34 \times 16 \times 0.25$ mm^3, Figure 1D(i)) using adhesive tape. Then, the GPA6 MSBC samples were inserted into a 3D-printed bottom-part mold ($40 \times 22 \times 1.5$ mm^3 with a socket of $36 \times 18 \times 0.4$ mm^3, Figure 1D(ii)) with alginate hydrogel (6% w/v, Protanal LF 10-60, FMC biopolymer) and covered with a dialysis cellulose membrane (MWCO 14000, Sigma-Aldrich, Israel) and then with the dedicated 3D-printed perforated top mold ($20 \times 38 \times 5$ mm with 162 holes of 1 mm diameter, Figure 1D(iii,iv)), and a small weight was placed on it to prevent the top mold from floating. The mold was sealed, flattened, and soaked in a 0.1 M $CaCl_2$ (Sigma-Aldrich, Israel) solution for at least 48 h at room temperature to cross-link the alginate and form a hydrogel matrix between the fibers (Figure 1D(v)). Collagen-alginate biocomposites were fabricated as described in our previous work.[37,41,42,44,45] In short, coral collagen fibers were extracted from the corals as described in Section 2.3 and then wrapped around thin rectangular frames. The arrayed collagen fiber frames were inserted into a dialysis membrane with a 6% w/v sodium alginate solution, as described for the MSBC biocomposite fabrication process.

2.5. Scanning Electron Microscopy. The nanofibers and the multiscale fibrous network samples were examined by a scanning electron microscope (SEM) (HRSEM Tescan MAIA 3) using a 5 kV voltage. The samples were sputtered with 10 nm of gold.

2.6. Fiber Fraction and Diameter. The nanofibers' diameter was computed from the SEM images of the electrospun film using the DiameterJ[46] plugins in the ImageJ software (NIH). Four different batches of GPA6 (3–9 different images per batch) and two different batches of PA6 (with 4–5 images per batch) were quantified.

For the MSBCs, the evaluated fiber volume fraction (FVF) was calculated as a volume quantification of collagen microfibers in the samples by multiplying the area fraction (AF) by the thickness ratio (TR). The AF of the collagen fibers was calculated by image analysis using MATLAB software. The AF was determined by processing the images of the frame with microfibers and calculating the percentage of white pixels (microfibers) from the dark background. The TR was determined as a ratio of the microfibers' thickness divided by the final thickness after adding the nanofibers. The collagen fibers' thickness was measured in several locations before and after the electrospinning process using a digital micrometer.

For the collagen-alginate and MSBC biocomposites, the FVF was calculated as previously described.[37,41,42,44,45] The FVF was determined as the normalized factor (NF) NF × AF × TR. The AF was determined as described for MSBC samples. For alginate-collagen biocomposites, the TR was determined as the ratio of the microfibers' thickness divided by the final thickness after adding the hydrogel matrix. For the MSBC biocomposites, the TR was determined as the ratio of the microfibers' thickness divided by the final thickness after electrospinning and adding hydrogel.

2.7. Mechanical Characterization. Unidirectional tensile testing was performed by a μTS load frame (Psylotech μTS system, IL) using 22 and 222 N load cells. The nanofibers and MSBC samples were cut and peeled from the aluminum foil using a scalpel. The average dimensions were used to calculate the cross-sectional area using a digital micrometer and a caliper. The cut samples were glued to the in-house 3D-printed frames using adhesive tape, where the microfibers in multiscale samples were aligned with the stretching direction. The samples were mounted to the tensile machine using custom-3D-printed clamps, and the gage length of each sample was measured as the distance between the clamps at zero force. Samples were stretched to failure at a rate of 1 mm/min using displacement control.

The mechanical properties were calculated as engineering stresses and strains: stresses were defined as the force divided by the initial cross-sectional area, and strains as the displacement divided by the initial gage length. The ultimate tensile strength (UTS) was defined as the maximum stress, and the maximum strain as the strain at UTS (ultimate strain). The moduli were calculated as the tangent modulus at a specific strain.

For the biocomposites, the samples were preconditioned for 5% strain for three cycles and then stretched to failure at a 3 mm/min rate using displacement control. The elastic modulus was calculated in the linear region (0.1–0.13 mm/mm strain), and the toughness was defined as the area under the stress–strain curve. It was calculated up to a reduction of 40% of UTS value using the trapezoidal rule in Excel software.

2.8. Structural Organization of Fibrous Components in the ECM of Soft Tissues. Revealing the structural organization of fibrous components in the ECM of soft tissues is a critical step toward better understanding their structure–function relationship, identifying their clinical role in health and disease conditions, and creating engineered analogue structures. We pioneered a method based on alkali digestion with sonication to visualize the ultrastructure of fibers (collagen and elastin) in the intervertebral disk (IVD),[47,48] which has led to the detection of fiber organization in different regions of IVD that was not reported previously.[49,50] This method was employed for ultrastructural analysis and biomechanical assessment of fibers leading to the fabrication of better tissue-engineered scaffolds. The simultaneous

https://doi.org/10.1021/acsapm.3c00057
ACS Appl. Polym. Mater. 2023, 5, 2816–2829

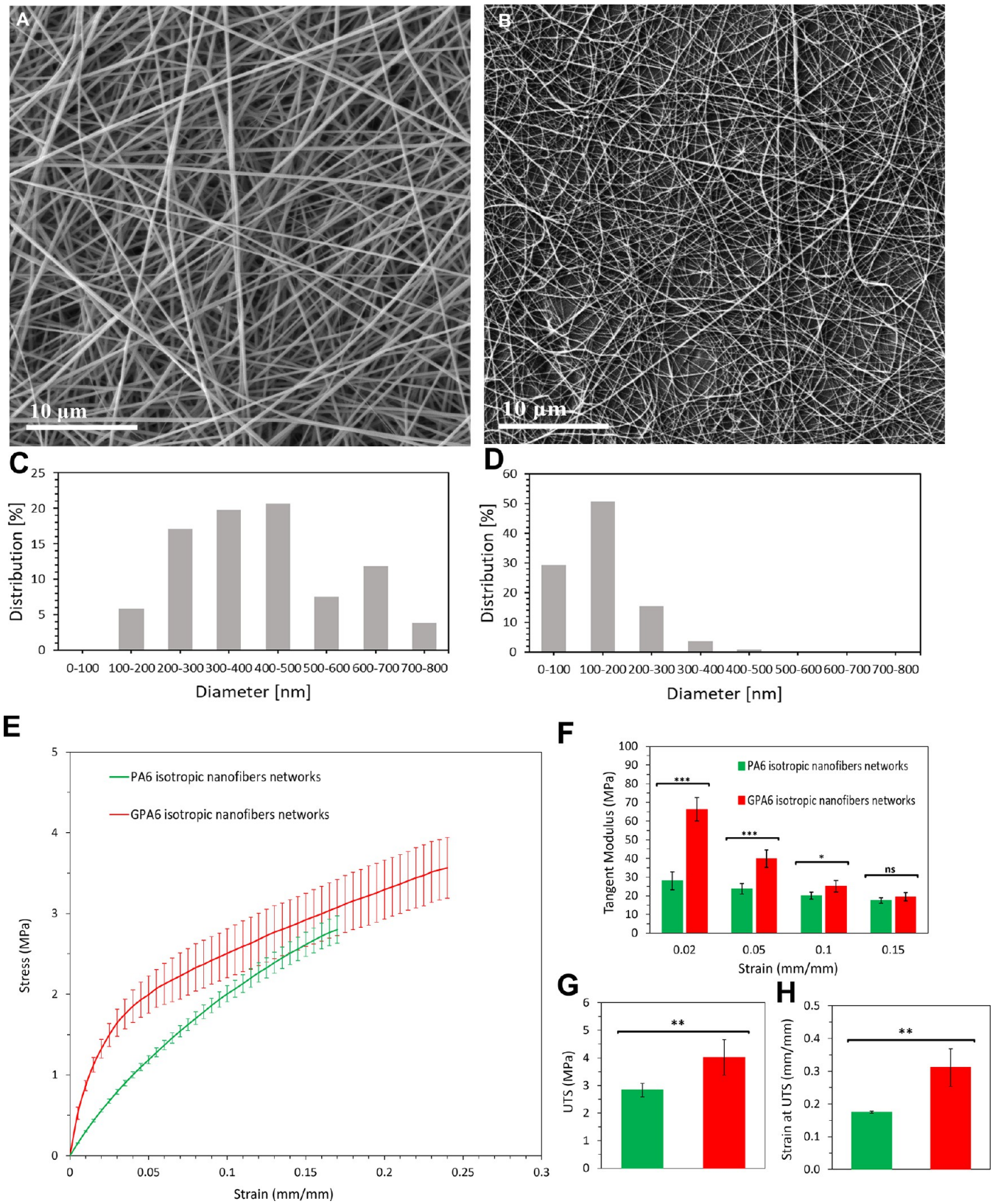

Figure 2. Isotropic nanofibrous networks: structure and mechanical behavior. Representative SEM images of (A) GPA6 and (B) PA6 nanofibers mats. Representative distribution of nanofibers diameter: (C) GPA6 and (D) PA6. (E) Stress−strain curves. (F) Tangent modulus in different strains. (G) Ultimate tensile strength. (H) Strain at UTS (*p < 0.05, **p < 0.005, ***p < 0.0005, and ****p < 0.0001).

sonication and alkali digestion of tissue allowed us to eliminate ECM components step by step. Thin tissue samples harvested from ovine IVDs were exposed to 0.5 M sodium hydroxide solution and sonication (25 kHz) for defined periods at room temperature. Post-heat treatment removed the IVD collagen fibers via gelatinization to visualize the arrangement of the elastic fibers. The samples were dried before SEM

https://doi.org/10.1021/acsapm.3c00057
ACS Appl. Polym. Mater. 2023, 5, 2816−2829

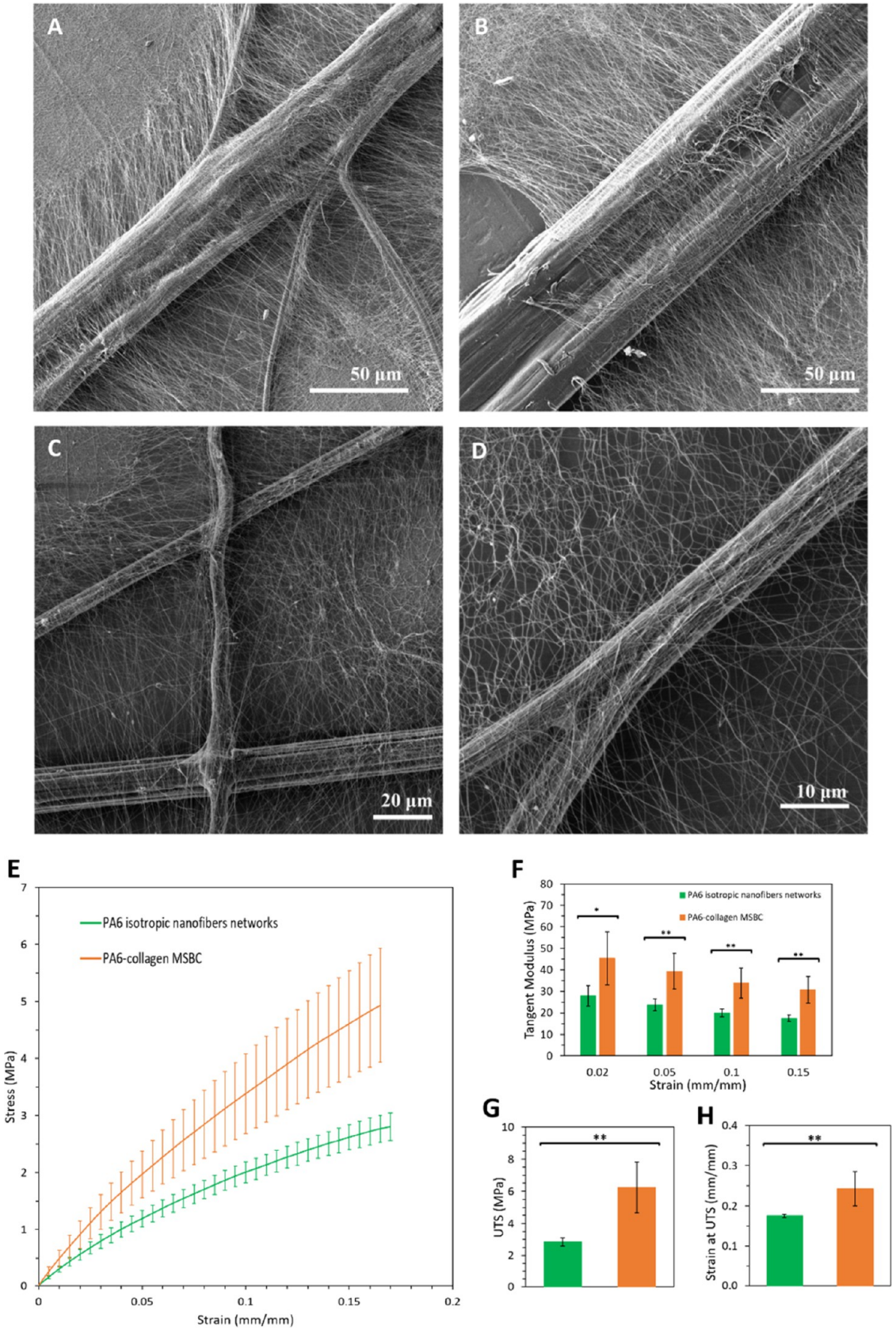

Figure 3. PA6-collagen MSBC structure and mechanical behavior. SEM images of (A, B) PA6 nanofibers mat covering the collagen bundles. (C, D) PA6 nanobridges among the collagen fibers. (E) Stress−strain curves. (F) Tangent Modulus comparison. (G) Ultimate tensile strength. (H) Strain at UTS.

https://doi.org/10.1021/acsapm.3c00057
ACS Appl. Polym. Mater. 2023, 5, 2816−2829

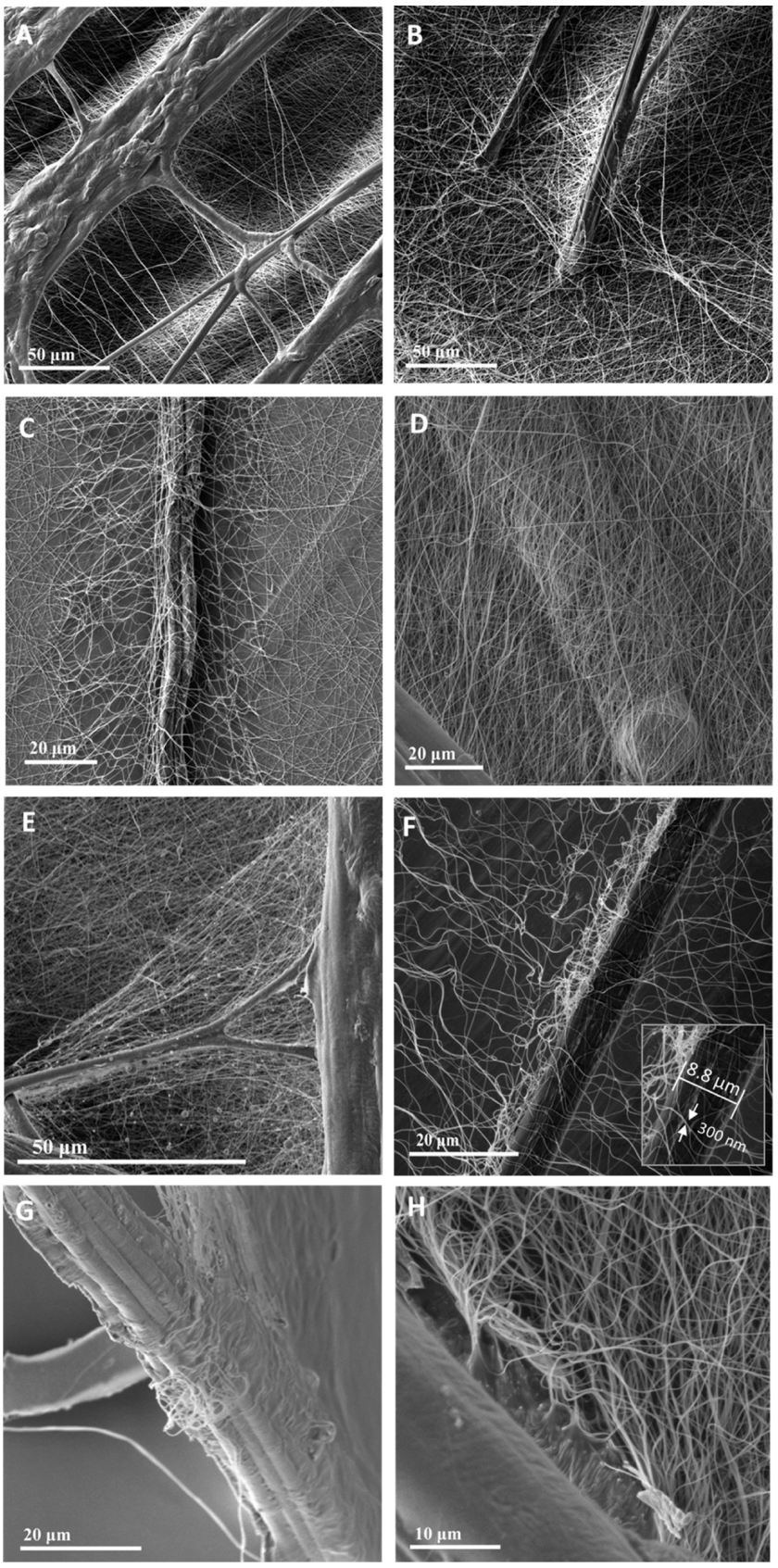

Figure 4. SEM images of GPA6-collagen MSBC structure. (A) GPA6 nanofibers network creates nanobridges among the collagen fibers. (B) Interface between the collagen microfibers and the nanofibers network mat. (C) 3D interface bonding. (D) Nanofibers network covers the collagen fiber. (E) Nanofibers network forms nanobridges among the collagen fibers. (F) Micro−nano differences in diameter. (G) Nanofibers wrap the collagen bundle. (H) Interface close-up between the nanofibers and microfiber.

https://doi.org/10.1021/acsapm.3c00057
ACS Appl. Polym. Mater. 2023, 5, 2816−2829

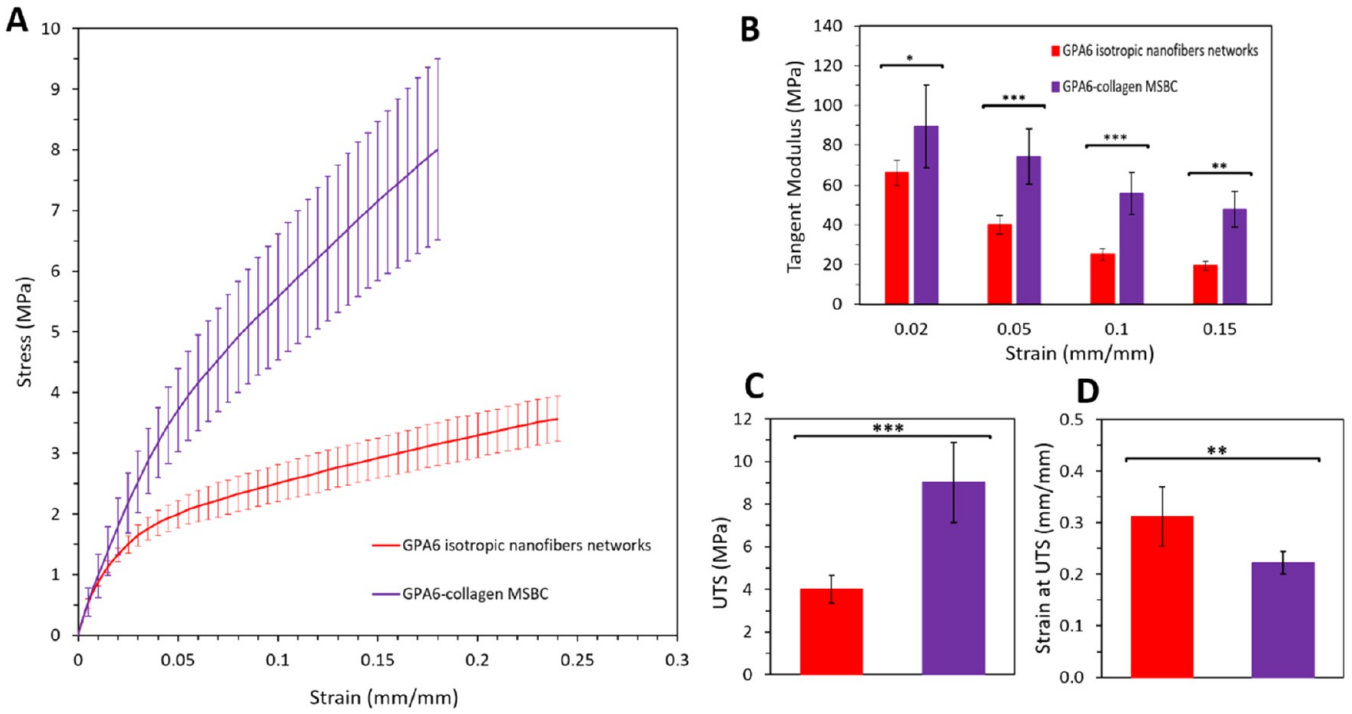

Figure 5. GPA6-collagen MSBC and GPA6 isotropic nanofibrous network mechanical properties. (A) Stress−strain curves. (B) Tangent modulus at different strains. (C) Ultimate tensile strength. (D) Strain at UTS.

imaging (Inspect F50, FEI Company) in a vacuum oven (VO3, LABEC, Australia) overnight at 37 °C and −80 kPa. Dried specimens were sputter coated with platinum at 2 nm.

2.9. Statistical Analysis. The mean and standard deviation (SD) were calculated for all measurements. Statistical analysis was performed using GraphPad Prism 9.4.1 software. The results with $p < 0.05$ were considered statistically significant. One-way ANOVA ($\alpha = 0.05$) with correction of Tukey test was used to compare the data groups.

3. RESULTS

3.1. PA6 and GPA6 Nanofibrous Mats. The fabrication process and geometry of the nonwoven nanofibers mats and multiscale biomimetic constructs (MSBCs) are presented in Figure 1 and Table 1.

Two types of isotropic nanofibers mats were fabricated (Figure 2A,B): PA6 (polyamide 6) and hybrid GPA6 (gelatin-polyamide 6). The average fiber diameter of the GPA6 (428.7 ± 162.8 nm) was significantly larger than PA6 (125.6 ± 37.8 nm) by 341%. Furthermore, the fiber diameter for isotropic GPA6 mats was broadly distributed (Figure 2C,D).

The material behavior of the nanofibrous mats was different: the initial slope of the GPA6 stress−strain curve was significantly stiffer than the PA6 (Figure 2E). The tangent moduli for the GPA6 were larger than the PA6. This difference was larger in small strain values ($p < 0.0005$, Figure 2F). UTS and the strain at UTS were larger for GPA6, at 142 and 172%, respectively ($p < 0.005$, Figure 2G,H).

3.2. PA6 MSBCs. Multiscale biomimetic constructs (MSBCs) of PA6-collagen were fabricated by combining the PA6 nanofibers by the electrospinning process with the aligned collagen microfibers (Figure 1C). The average diameter of the collagen microfibers (9.4 ± 3.0 μm) was larger than PA6 nanofibrous diameter (125.6 ± 37.8 nm) in ∼2 orders of magnitude. The differences in diameter are remarkably seen in Figure 3: the collagen microfibers are shown as bundles and fibers (Figure 3B,C, respectively). The electrospun nanofibers created a mat that covers the collagen fibers (Figure 3A,B). A nanobridges structure was formed among the collagen fibers (Figure 3C,D).

The mechanical behavior of the PA6-collagen MSBC (FVF 12%) was significantly stiffer than PA6 nanofibrous samples (Figure 3E). The tangent moduli comparison demonstrated that the PA6-collagen MSBC was significantly stiffer than the PA6 nanofibrous for all strain values ($p < 0.005$, Figure 3F). This difference was more significant in strains larger than 0.02 mm/mm. Moreover, the UTS and the strain at UTS were significantly larger for MSBC PA6-collagen than for PA6 nanofibrous samples, at 220% (6.2 ± 1.6 and 2.8 ± 0.2 MPa, respectively) and 141% (0.24 ± 0.04 and 0.17 ± 0.00, respectively) ($p < 0.005$, Figure 3G,H).

3.3. GPA6 MSBCs. MSBCs of GPA6-collagen were fabricated as described for the PA6-collagen MSBC. The average diameter of the collagen microfibers (9.4 ± 3.0 μm) was ∼22 times larger than the GPA6 nanofibrous diameter (428.7 ± 162.8 nm) (Figure 4). The micro−nano differences in diameter are highlighted in Figure 4F. It was shown that the structure is characterized in nanobridges by the electrospun nanofibers among the collagen fibers (Figure 4A,E). Moreover, the collagen microfibers were wrapped by the electrospun GPA6 nanofibers (Figure 4D,G), and the interface and bonding between the two scales of materials were seen clearly (Figure 4B,C,H).

The mechanical behavior of the GPA6-collagen MSBC (FVF 15%) was significantly stiffer than GPA6 nanofibrous samples (Figure 5A). The tangent moduli comparison demonstrated that the GPA6-collagen MSBC was significantly stiffer than the GPA6 nanofibers (Figure 5B). This difference was more significant in 0.05 and 0.1 mm/mm strains. Moreover, the UTS was significantly larger for the GPA6-collagen MSBC than for GPA6 nanofibrous samples, at 224% (9.0 ± 1.9 and 4.0 ± 0.6 MPa, respectively, $p < 0.0005$, Figure 5C), but the strain at UTS

https://doi.org/10.1021/acsapm.3c00057
ACS Appl. Polym. Mater. 2023, 5, 2816−2829

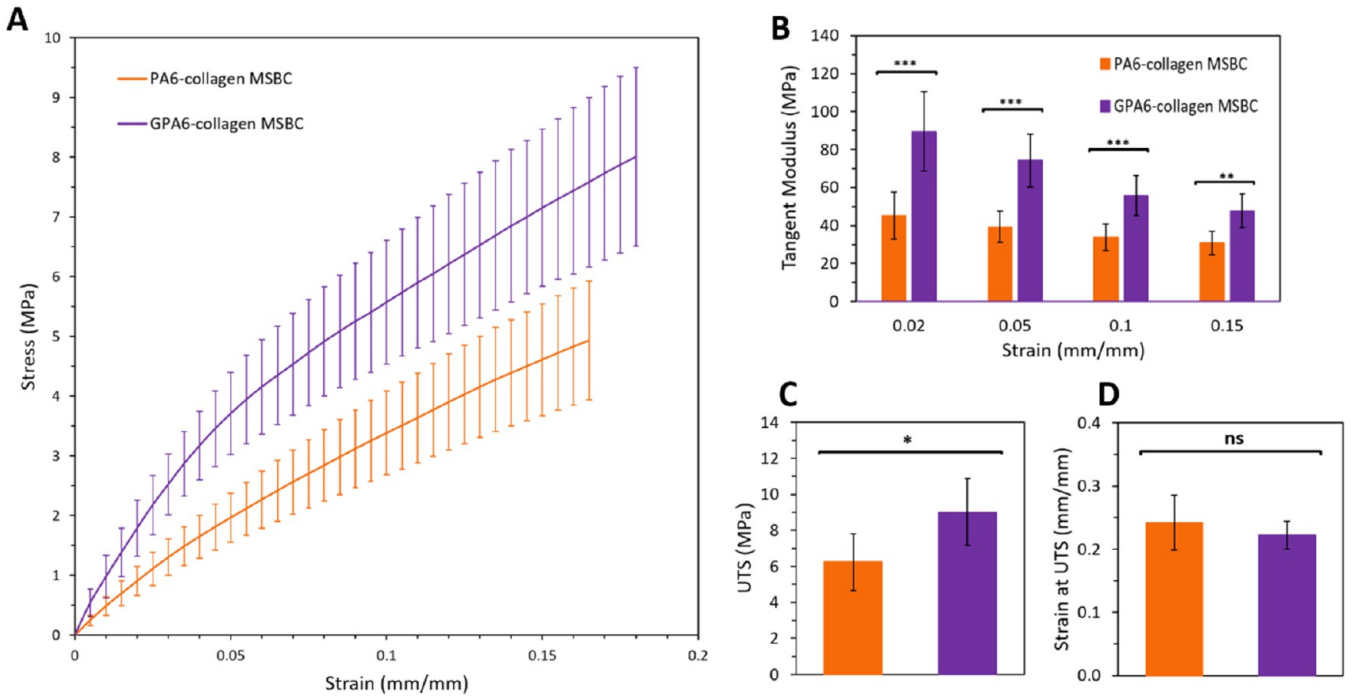

Figure 6. GPA6-collagen MSBC and PA6-collagen MSBC mechanical properties. (A) Stress−strain curves. (B) Tangent Modulus in different strains. (C) Ultimate tensile strength. (D) Strain at UTS.

was lower than the GPA6 at 141% (0.22 ± 0.02 and 0.31 ± 0.06, respectively) ($p < 0.005$, Figure 5D).

The GPA6-collagen MSBC was stiffer than the PA6-collagen MSBC (Figure 6A). The tangent moduli were significantly larger for the GPA6-collagen MSBC than the PA6-collagen MSBC, especially at strains up to 0.1 mm/mm ($p < 0.0005$, Figure 6B). The UTS of the GPA6-collagen is larger than the PA6-collagen at 145% (9.0 ± 1.9 and 6.2 ± 1.6 MPa, $p < 0.05$, Figure 6C), while the strain at UTS was not significantly different between the two MSBC materials ($p = 0.278$, Figure 6D).

3.4. GPA6 MSBC Biocomposites. GPA6 MSBCs were chosen for creating biocomposites due to their enhanced mechanical properties and better structural interactions within the multiscale structure. The MSBC biocomposites demonstrated a different behavior than the GPA6 MSBCs (Figure 7A). Although less stiff, the MSBC biocomposites presented a nonlinear behavior with strain stiffening and large deformations. Compared to collagen-alginate biocomposites (FVF 0.2, 0.3), the MSBC biocomposites demonstrated significantly larger strain at UTS and toughness ($p < 0.0001$ and $p < 0.0005$, respectively, Figure 7C,E). The MSBC biocomposites demonstrated great mechanical compatibility with different human soft tissues: meniscus (radial orientation),[51] aortic valve (circumferential orientation),[52] annulus fibrosus (circumferential orientation),[53] and cornea.[54]

4. DISCUSSION

The fibrous network structure and its components are vital for the functionality of soft tissues. The current study aims to investigate the fabrication of multiscale nano-to-micro constructs and biocomposites and characterize their structure and mechanical behavior. Herein, we fabricated different material systems and characterized the mechanical and structural properties step by step as a standalone component to isolate their role and up to a whole micro−nano multiscale biocomposite.

Gelatin is a soluble protein obtained by partial hydrolysis of collagen[55] and has a similar composition of amino acids as collagen.[56] Polyamide 6 is a synthetic hydrophilic polymer, similar to proteins that are naturally occurring polyamides such as collagen, wool, and silk.[57,58] Its biocompatible properties stem from the presence of amide groups. These groups share a similar chemical structure with natural peptides. Therefore, it can deceive the immune system and have low immunogenicity.

Furthermore, PA6 is simple to electrospun and has excellent flexibility and high tensile strength. It creates hydrogen bonds that stabilize its structure.[36,58,59] Therefore, we hypothesized that as a reinforcement hydrated matrix, it would enable weak hydrophilic noncovalent interactions. These interactions, together with the immense inherent PA6 flexibility, will allow reversible binding and large deformations as in natural soft tissues.[9,12,36,44,60,61]

Although it has poor biodegradability capacity as raw material, it can be improved.[62] Alginate hydrogel is a negatively charged polysaccharide that absorbs water, providing aqueous surroundings to the biocomposites and allowing weak and reversible interactions with collagen and nylon fibers.[36,37,39−42] The coral collagen microfibers demonstrated biological compatibility and fantastic mechanical and structural properties, including nonlinear hyperelastic behavior, large stiffness and strength, and inherent crimping with great potential in soft tissue engineering, with minimal processing intervention.[37−40,42,63] The biocompatibility of the coral collagen fibers and their alginate-based composites was previously studied. The seeded cells demonstrated oriented growth on the coral collagen fibers for 40 days.[37,38,63] Gelatin and PA6 and their combination were also widely investigated for their biocompatibility and tissue-engineering applications.[35,64−68]

The PA6 and GPA6 electrospun nanofibers demonstrated different fiber diameters and mechanical properties (Figure 2).

https://doi.org/10.1021/acsapm.3c00057
ACS Appl. Polym. Mater. 2023, 5, 2816−2829

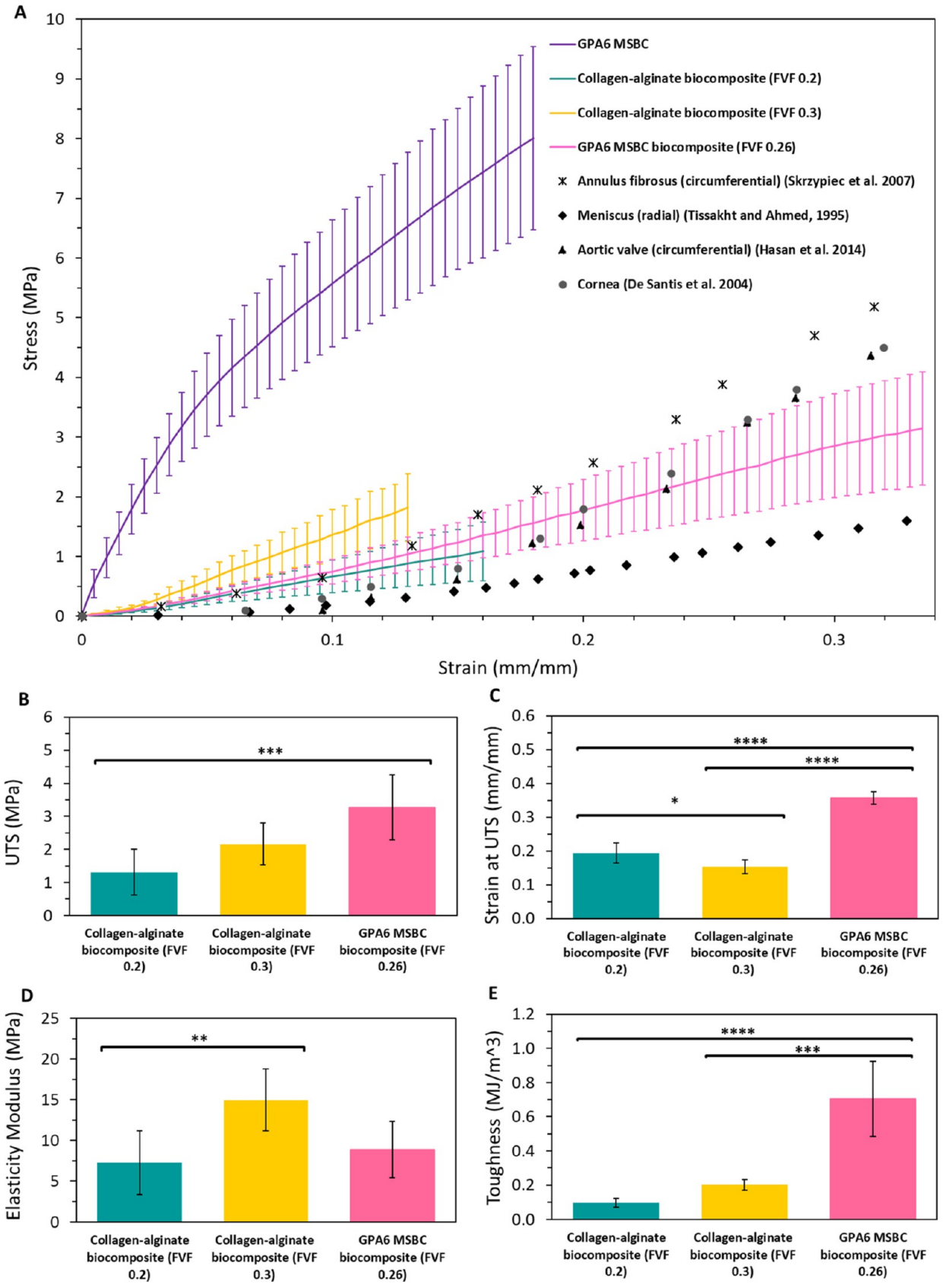

Figure 7. (A) Mechanical behavior of GPA6-collagen MSBC, GPA6-collagen-alginate MSBC biocomposites, collagen-alginate biocomposites, and human tissues: meniscus (radial orientation),[51] aortic valve (circumferential orientation),[52] annulus fibrosus (circumferential orientation),[53] and cornea.[54] Mechanical properties of alginate-collagen biocomposites and MSBC biocomposites: (B) ultimate tensile strength, (C) strain at UTS, (D) modulus, and (E) toughness.

https://doi.org/10.1021/acsapm.3c00057
ACS Appl. Polym. Mater. 2023, 5, 2816−2829

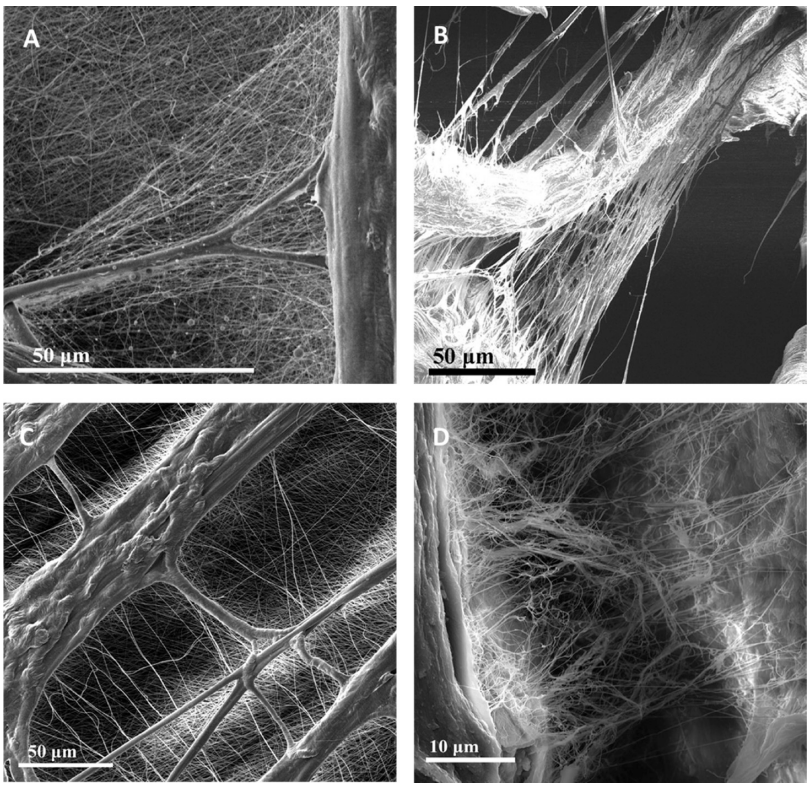

Figure 8. GPA6-collagen MSBC structure (A, C) compared with the native elastic fibrous network in (B, D) an ovine intervertebral disk.

The addition of gelatin to the GPA6 significantly influenced both structural and mechanical properties, as previously described.[69,70]

The overall structure of both MSBCs exhibited an entangled structure composed of micro and nanofibrous network, including nanobridges that connected the microfibers (Figures 3D and 4E). The collagen microfibers significantly strengthen the nanofibrous mats. This feature indicates binding between the two scales of materials in addition to the organization feature.

The collagen-GPA6 MSBC demonstrated better interactions between the different scales, where the nanofibers were clearly attached to the collagen microfibers, and the interface was visible. The improved interface was probably due to the gelatin-collagen chemical similarity, unlike the collagen-PA6 MSBCs that demonstrated fewer interactions (Figures 3 and 4).

In both cases, the MSBCs demonstrated improved tangent moduli and UTS compared with the nanofibers mats. However, in the collagen-PA6 MSBC, the strain at UTS was improved as well, unlike the collagen-GPA6 MSBC (Figures 3, 5, and 6). That behavior may indicate that the chemical connection between the collagen and PA6 may be strong, and the PA6 nanofibers have significantly ductile behavior. That is not the case for the collagen-GPA6 MSBC. However, when comparing the MSBCs, the difference in the max strains is negligible, but UTS and moduli are larger for the GPA6 MSBC, which makes the combined structure stiffer and stronger.

The MSBC biocomposites are composed of combined micro and nanofiber structures embedded in alginate hydrogel. The hydrated nature of the hydrogel generates weak interactions in the interface between the fibers and matrix. These weak interactions allow the nonlinear behavior with strain stiffening and large deformations, as seen for the collagen-alginate biocomposites (Figure 7).[37,41,42,44,45] The MSBC biocomposites demonstrated even larger strains and toughness due to the presence of the nanofibers and cross-bridges. On the one hand, the addition of the nanofibers to the collagen microfibers biocomposites resulted in significantly larger strains and toughness.

On the other hand, adding aqueous surroundings (the hydrogel matrix) significantly changed the mechanical behavior of the MSBC to resemble native soft tissue behavior by activating additional structural mechanisms such as sliding and straightening of the fibers. The sliding of the nano and microfibers is attributed to the hydrogen bonds formed between the hydrophilic fibers and matrix, allowing reverse interactions and sliding. Moreover, the straightening of micro crimping is responsible for the toe region and strain stiffening behavior that occurs due to the hydrophilic composite nature of our structures, as in native soft tissues.[9,71−73]

Furthermore, MSBC biocomposites showed considerable similarity with the mechanical behavior of human tissues as the meniscus (radial orientation),[51] aortic valve (circumferential orientation),[52] annulus fibrosus (circumferential orientation),[53] and cornea.[54] The common ground for all of these tissues in their specific orientations is not their stiffness and strength but their ability to withstand large deformations under complex loading modes and to maintain tissue durability.

We have recently shown similar behavior of hierarchical structure made of nanofibers embedded in a soft hydrogel matrix, with increased strain and toughness.[36] Therefore, we can conclude that the addition of the nanofibers creates additional inherent networks in the composites that increase strain and toughness, as in native soft tissues. Moreover, and very importantly, nanoscale reinforcement is known to simultaneously favor the strength and toughness of materials.[74,75]

https://doi.org/10.1021/acsapm.3c00057
ACS Appl. Polym. Mater. 2023, 5, 2816−2829

Therefore, incorporating multiscale biocomposites is essential for large deformations and increased toughness, as also demonstrated by Yao et al.[76]

The addition of the nanofibers to the biocomposite confirmed their significant role in the overall structure. These structures showed significant improvement in toughness, max strains, and UTS, which are crucial for soft tissue analogues. Furthermore, the presence of water, provided by the alginate hydrogel matrix, is essential for the mechanical behavior of soft tissue analogues due to the formation of hydrophilic interactions that govern the hyperelastic behavior of the biocomposites and soft tissues.[9] Thus, the hydrogel is essential for the hydration of the 3D fibrous networks[77] and is mechanically equivalent to the GAGs in the native tissues.[78]

The collagen-GPA6 MSBC (Figure 8A,C) demonstrated remarkable similarity to the native fibrous networks' hierarchical structure (Figure 8B,D). The latter is characterized by a fibrous nano−micro configuration of the elastic fibers in ovine intervertebral disks (Figure 8B,D). This native ultrastructural organization also creates entangled elastic networks in other soft tissues.[79] The elastic network essentially allows tissue durability by providing flexibility, recoiling ability, and fatigue resistance.[9] Furthermore, the nanofibers network contributes intrinsic compressive stresses to the collagen fibers and enables the collagen fibers to recoil.[80] This connection of the microfibers with the nanofibers network improves the mechanical properties.[81,82] The elastic fibers, which are found in the native fibrous networks in soft tissues such as skin, lungs, and arteries, vary in fiber diameter, orientation, and distribution. However, collagen−elastin interfaces demonstrated similar arrangements in different tissues.[83,84] These elastic fiber networks enable the tissue to withstand large stretches without tearing for a long time.[9,85] Native fibrous networks have unique arrangements and architectures destined to hold varied local mechanical stresses that can be controlled due to the spatial arrangement of the nanofibers.[86] Therefore, fabricating different analogues should consider the influence of these structures' variability and their influence on the overall structure.[87]

It is important to note that the 3D ECM fiber networks also have an additional important role in modulating cell function. Thus, multiscale micro−nano fibers also have a biological role: to induce desired cellular activities and guide 3D tissue regeneration.[88]

This study demonstrated the fabrication of biomimetic multiscale micro−nano constructs and their mechanical and structural characterization for the construction of soft tissue analogues. Different combinations of the material systems can induce varied microenvironments for different local properties. Our material system has the potential to be used for the next-generation tissue repair and replacement applications.

5. CONCLUSIONS

Herein, we have demonstrated a simple method for fabricating multiscale biomimetic composites. We investigated the step-by-step influence of different components on the structure−mechanical function relationship. We have demonstrated structural binding between the different length scales in our MSBCs, and the importance of material selection that improved the adhesion between the scales due to the chemical similarity of the MSBC components. The collagen microfibers increased the stiffness and UTS, whereas the nanofibers improved the ductility, toughness, and large deformations. The collagen-GPA6 MSBC also demonstrated remarkable structural similarity to the native fibrous network structures in soft tissues. Furthermore, incorporating the alginate hydrogel into the construct remarkably improved the mechanical compatibility with native soft tissues by adding water to the material system and allowing increased toughness, large deformations, and strain stiffening. Our results present material constructs that can be utilized for biomimetic tailor-designed specialized structures for soft tissue repair and replacement.

AUTHOR INFORMATION

Corresponding Author

Mirit Sharabi − *Department of Mechanical Engineering and Mechatronics, Ariel University, Ariel 407000, Israel;* orcid.org/0000-0003-4421-154X; Phone: +972-3-6453159; Email: miritsh@ariel.ac.il

Authors

Smadar E. Sharon − *Department of Mechanical Engineering and Mechatronics, Ariel University, Ariel 407000, Israel*

Adi Aharonov − *Department of Mechanical Engineering and Mechatronics, Ariel University, Ariel 407000, Israel*

Haim S. Mordechai − *Department of Mechanical Engineering and Mechatronics, Ariel University, Ariel 407000, Israel*

Javad Tavakoli − *School of Biomedical Engineering, University of Technology Sydney, Sydney, NSW 2007, Australia*

Complete contact information is available at: https://pubs.acs.org/10.1021/acsapm.3c00057

Author Contributions

The manuscript was written through contributions of all authors. All authors have given approval to the final version of the manuscript.

Notes

The authors declare no competing financial interest.

ACKNOWLEDGMENTS

The authors thank Prof. Rami Haj-Ali for the soft coral donation. The authors are thankful to Ariel University for its financial support. Also, this research was partly supported by the Israel Science Foundation (Grant 1424/22).

ABBREVIATIONS

PA6, polyamide 6; GPA6, gelatin-polyamide 6; FVF, fiber volume fraction; MSBCs, multiscale biomimetic constructs; UTS, ultimate tensile strength

REFERENCES

(1) Causa, F.; Netti, P. A.; Ambrosio, L. A Multi-Functional Scaffold for Tissue Regeneration: The Need to Engineer a Tissue Analogue. *Biomaterials* **2007**, *28*, 5093−5099.

(2) Bhattarai, N.; Li, Z.; Edmondson, D.; Zhang, M. Alginate-Based Nanofibrous Scaffolds: Structural, Mechanical, and Biological Properties. *Adv. Mater.* **2006**, *18*, 1463−1467.

(3) Mauck, R. L.; Baker, B. M.; Nerurkar, N. L.; Burdick, J. A.; Li, W.-J.; Tuan, R. S.; Elliott, D. M. Engineering on the Straight and Narrow: The Mechanics of Nanofibrous Assemblies for Fiber-Reinforced Tissue Regeneration. *Tissue Eng., Part B* **2009**, *15*, 171−193.

(4) Rizvi, M. S.; Kumar, P.; Katti, D. S.; Pal, A. Mathematical Model of Mechanical Behavior of Micro/Nanofibrous Materials Designed for Extracellular Matrix Substitutes. *Acta Biomater.* **2012**, *8*, 4111−4122.

(5) Eisner, L. E.; Rosario, R.; Andarawis-Puri, N.; Arruda, E. M. The Role of the Non-Collagenous Extracellular Matrix in Tendon and Ligament Mechanical Behavior: A Review. *J. Biomech. Eng.* **2022**, *144*, No. 050801.

(6) Xiang, T.; Hou, J.; Xie, H.; Liu, X.; Gong, T.; Zhou, S. Biomimetic Micro/Nano Structures for Biomedical Applications. *Nano Today* **2020**, *35*, No. 100980.
(7) Jung, G. S.; Buehler, M. J. Multiscale Modeling of Muscular-Skeletal Systems. *Annu. Rev. Biomed. Eng.* **2017**, *19*, 435−457.
(8) Mazza, E.; Ehret, A. E. Mechanical Biocompatibility of Highly Deformable Biomedical Materials. *J. Mech. Behav. Biomed. Mater.* **2015**, *48*, 100−124.
(9) Sharabi, M. Structural Mechanisms in Soft Fibrous Tissues: A Review. *Front. Mater.* **2022**, *8*, No. 793647.
(10) Tuzlakoglu, K.; Bolgen, N.; Salgado, A. J.; Gomes, M. E.; Piskin, E.; Reis, R. L. Nano- and Micro-Fiber Combined Scaffolds: A New Architecture for Bone Tissue Engineering. *J. Mater. Sci. Mater. Med.* **2005**, *16*, 1099−1104.
(11) Shoulders, M. D.; Raines, R. T. Collagen Structure and Stability. *Annu. Rev. Biochem.* **2009**, *78*, 929−958.
(12) Yang, W.; Meyers, M. A.; Ritchie, R. O. Structural Architectures with Toughening Mechanisms in Nature: A Review of the Materials Science of Type-I Collagenous Materials. *Prog. Mater. Sci.* **2019**, *103*, 425−483.
(13) Fratzl, P. *Collagen: Strucure and Mechanics, An Introduction*; Springer: Boston, MA, 2008; Vol. *148*.
(14) Scott, J. E.; Orford, C. R.; Hughes, E. W. Proteoglycan-Collagen Arrangements in Developing Rat Tail Tendon. *Biochem. J.* **1981**, *195*, 573−581.
(15) Debelle, L.; Tamburro, A. M. Elastin: Molecular Description and Function. *Int. J. Biochem. Cell Biol.* **1999**, *31*, 261−272.
(16) Moller, M.; Matyjaszewski, K. *Polymer Science: A Comprehensive Reference*; Elsevier, 2012; Vol. *1*.
(17) Cyril, D.; Giugni, A.; Bangar, S. S.; Mirzaeipoueinak, M.; Shrivastav, D.; Sharabi, M.; Tipper, J. L.; Tavakoli, J. Elastic Fibers in the Intervertebral Disc: From Form to Function and toward Regeneration. *Int. J. Mol. Sci.* **2022**, *23*, 8931.
(18) Karsdal, M. A.; Leeming, D. J.; Henriksen, K.; Bay-Jensen, A. C. *Biochemistry of Collagens, Laminins and Elastin: Structure, Function and Biomarkers*; Elsevier B.V., 2016.
(19) Tavakoli, J.; Costi, J. J. New Insights into the Viscoelastic and Failure Mechanical Properties of the Elastic Fiber Network of the Inter-Lamellar Matrix in the Annulus Fibrosus of the Disc. *Acta Biomater.* **2018**, *77*, 292−300.
(20) Quantock, A. J.; Winkler, M.; Parfitt, G. J.; Young, R. D.; Brown, D. J.; Boote, C.; Jester, J. V. From Nano to Macro: Studying the Hierarchical Structure of the Corneal Extracellular Matrix. *Exp. Eye Res.* **2015**, *133*, 81−99.
(21) Kong, B.; Liu, R.; Guo, J.; Lu, L.; Zhou, Q.; Zhao, Y. Tailoring Micro/Nano-Fibers for Biomedical Applications. *Bioact. Mater.* **2023**, *19*, 328−347.
(22) Nam, Y. S.; Park, T. G. Porous Biodegradable Polymeric Scaffolds Prepared by Thermally Induced Phase Separation. *J. Biomed. Mater. Res.* **1999**, *47*, 8−17.
(23) Wu, X.; Liu, Y.; Li, X.; Wen, P.; Zhang, Y.; Long, Y.; Wang, X.; Guo, Y.; Xing, F.; Gao, J. Preparation of Aligned Porous Gelatin Scaffolds by Unidirectional Freeze-Drying Method. *Acta Biomater.* **2010**, *6*, 1167−1177.
(24) Nocera, A. D.; Comín, R.; Salvatierra, N. A.; Cid, M. P. Development of 3D Printed Fibrillar Collagen Scaffold for Tissue Engineering. *Biomed. Microdevices* **2018**, *20*, 26.
(25) Murphy, S. V.; Atala, A. 3D Bioprinting of Tissues and Organs. *Nat. Biotechnol.* **2014**, *32*, 773−785.
(26) Guo, J.; Yu, Y.; Zhang, D.; Zhang, H.; Zhao, Y. Morphological Hydrogel Microfibers with MXene Encapsulation for Electronic Skin. *Research* **2021**, *2021*, No. 7065907.
(27) Shalumon, K. T.; Chennazhi, K. P.; Tamura, H.; Kawahara, K.; Nair, S. V.; Jayakumar, R. Fabrication of Three-Dimensional Nano, Micro and Micro/Nano Scaffolds of Porous Poly(Lactic Acid) by Electrospinning and Comparison of Cell Infiltration by Z-Stacking/Three-Dimensional Projection Technique. *IET Nanobiotechnol.* **2012**, *6*, 16−25.
(28) Pham, Q. P.; Sharma, U.; Mikos, A. G. Electrospinning of Polymeric Nanofibers for Tissue Engineering Applications: A Review. *Tissue Eng.* **2006**, *12*, 1197−1211.
(29) Kim, S. J.; Jang, D. H.; Park, W. H.; Min, B. M. Fabrication and Characterization of 3-Dimensional PLGA Nanofiber/Microfiber Composite Scaffolds. *Polymer* **2010**, *51*, 1320−1327.
(30) Liu, L.; Kamei, K.; Yoshioka, M.; Nakajima, M.; Li, J.; Fujimoto, N.; Terada, S.; Tokunaga, Y.; Koyama, Y.; Sato, H.; Hasegawa, K.; Nakatsuji, N.; Chen, Y. Nano-on-Micro Fibrous Extracellular Matrices for Scalable Expansion of Human ES/IPS Cells. *Biomaterials* **2017**, *124*, 47−54.
(31) Yu, C.; Guan, G.; Glas, S.; Wang, L.; Li, Z.; Turng, L. S. A Biomimetic Basement Membrane Consisted of Hybrid Aligned Nanofibers and Microfibers with Immobilized Collagen IV and Laminin for Rapid Endothelialization. *Bio-Des. Manuf.* **2021**, *4*, 171−189.
(32) Yang, Z.; Peng, H.; Wang, W.; Liu, T. Crystallization Behavior of Poly(ε-Caprolactone)/Layered Double Hydroxide Nanocomposites. *J. Appl. Polym. Sci.* **2010**, *116*, 2658−2667.
(33) Tuzlakoglu, K.; Santos, M. I.; Neves, N.; Reis, R. L. Design of Nano- and Microfiber Combined Scaffolds by Electrospinning of Collagen onto Starch-Based Fiber Meshes: A Man-Made Equivalent of Natural Extracellular Matrix. *Tissue Eng., Part A* **2011**, *17*, 463−473.
(34) Xu, Y.; Shi, G.; Tang, J.; Cheng, R.; Shen, X.; Gu, Y.; Wu, L.; Xi, K.; Zhao, Y.; Cui, W.; Chen, L. ECM-Inspired Micro/Nanofibers for Modulating Cell Function and Tissue Generation. *Sci. Adv.* **2020**, *6*, No. eabc2036.
(35) Kong, B.; Chen, Y.; Liu, R.; Liu, X.; Liu, C.; Shao, Z.; Xiong, L.; Liu, X.; Sun, W.; Mi, S. Fiber Reinforced GelMA Hydrogel to Induce the Regeneration of Corneal Stroma. *Nat. Commun.* **2020**, *11*, No. 1435.
(36) Sharabi, M.; Wagner, H. D. Structural Biomimetics in Soft Synthetic Composite Materials: A Proof-of-Concept Alginate-Polyamide Soft Hierarchical Composite. *eXPRESS Polym. Lett.* **2021**, *15*, 708−724.
(37) Wertheimer, S.; Sharabi, M.; Shelah, O.; Lesman, A.; Haj-Ali, R. Bio-Composites Reinforced with Unique Coral Collagen Fibers: Towards Biomimetic-Based Small Diameter Vascular Grafts. *J. Mech. Behav. Biomed. Mater.* **2021**, *119*, No. 104526.
(38) Benayahu, D.; Sharabi, M.; Pomeraniec, L.; Awad, L.; Haj-Ali, R.; Benayahu, Y. Unique Collagen Fibers for Biomedical Applications. *Mar. Drugs* **2018**, *16*, 102.
(39) Sharabi, M.; Wertheimer, S.; Wade, K. R.; Galbusera, F.; Benayahu, D.; Wilke, H.-J.; Haj-Ali, R. Towards Intervertebral Disc Engineering: Bio-Mimetics of Form and Function of the Annulus Fibrosus Lamellae. *J. Mech. Behav. Biomed. Mater.* **2019**, *94*, 298−307.
(40) Sharabi, M.; Varssano, D.; Eliasy, R.; Benayahu, Y.; Benayahu, D.; Haj-Ali, R. Mechanical Flexure Behavior of Bio-Inspired Collagen-Reinforced Thin Composites. *Compos. Struct.* **2016**, *153*, 392−400.
(41) Sharabi, M.; Mandelberg, Y.; Benayahu, D.; Benayahu, Y.; Azem, A.; Haj-Ali, R. A New Class of Bio-Composite Materials of Unique Collagen Fibers. *J. Mech. Behav. Biomed. Mater.* **2014**, *36*, 71−81.
(42) Sharabi, M.; Benayahu, D.; Benayahu, Y.; Isaacs, J.; Haj-Ali, R. Laminated Collagen-Fiber Bio-Composites for Soft-Tissue Bio-Mimetics. *Compos. Sci. Technol.* **2015**, *117*, 268−276.
(43) Suki, B. Introduction to Structure-Function Relationships. *Struct. Funct. Extracell. Matrix* **2022**, 1−7.
(44) Sharabi, M.; Varssano, D.; Eliasy, R.; Benayahu, Y.; Benayahu, D.; Haj-Ali, R. Mechanical Flexure Behavior of Bio-Inspired Collagen-Reinforced Thin Composites. *Compos. Struct.* **2016**, *153*, 392−400.
(45) Sharabi, M.; Wertheimer, S.; Wade, K. R.; Galbusera, F.; Benayahu, D.; Wilke, H.-J.; Haj-Ali, R. Towards Intervertebral Disc Engineering: Bio-Mimetics of Form and Function of the Annulus Fibrosus Lamellae. *J. Mech. Behav. Biomed. Mater.* **2019**, *94*, 298−307.
(46) Hotaling, N. A.; Bharti, K.; Kriel, H.; Simon, C. G. DiameterJ: A Validated Open Source Nanofiber Diameter Measurement Tool. *Biomaterials* **2015**, *61*, 327−338.

https://doi.org/10.1021/acsapm.3c00057
ACS Appl. Polym. Mater. 2023, 5, 2816−2829

(47) Tavakoli, J.; Costi, J. J. Development of a Rapid Matrix Digestion Technique for Ultrastructural Analysis of Elastic Fibers in the Intervertebral Disc. *J. Mech. Behav. Biomed. Mater.* **2017**, *71*, 175−183.
(48) Tavakoli, J.; Costi, J. J. A Method for Visualization and Isolation of Elastic Fibres in Annulus Fibrosus of the Disc. *Mater. Sci. Eng. C* **2018**, *93*, 299−304.
(49) Tavakoli, J.; Diwan, A. D.; Tipper, J. L. The Ultrastructural Organization of Elastic Fibers at the Interface of the Nucleus and Annulus of the Intervertebral Disk. *Acta Biomater.* **2020**, *114*, 323−332.
(50) Tavakoli, J.; Diwan, A. D.; Tipper, J. L. Elastic Fibers: The Missing Key to Improve Engineering Concepts for Reconstruction of the Nucleus Pulposus in the Intervertebral Disc. *Acta Biomater.* **2020**, *113*, 407−416.
(51) Tissakht, M.; Ahmed, A. M. Tensile Stress-Strain Characteristics of the Human Meniscal Material. *J. Biomech.* **1995**, *28*, 411−422.
(52) Hasan, A.; Ragaert, K.; Swieszkowski, W.; Selimović, Š.; Paul, A.; Camci-Unal, G.; Mofrad, M. R. K.; Khademhosseini, A. Biomechanical Properties of Native and Tissue Engineered Heart Valve Constructs. *J. Biomech.* **2014**, *47*, 1949−1963.
(53) Skrzypiec, D.; Tarala, M.; Pollintine, P.; Dolan, P.; Adams, M. A. When Are Intervertebral Discs Stronger than Their Adjacent Vertebrae? *Spine* **2007**, *32*, 2455−2461.
(54) De Santis, R.; Sarracino, F.; Mollica, F.; Netti, P. A.; Ambrosio, L.; Nicolais, L. Continuous Fibre Reinforced Polymers as Connective Tissue Replacement. *Compos. Sci. Technol.* **2004**, *64*, 861−871.
(55) Gómez-Guillén, M.; Gimenez, B.; Lopez-Caballero, M. E.; Montero, M. P. Functional and Bioactive Properties of Collagen and Gelatin from Alternative Sources: A Review. *Food Hydrocolloids* **2011**, *25*, 1813−1827.
(56) Tylingo, R.; Gorczyca, G.; Mania, S.; Szweda, P.; Milewski, S. Preparation and Characterization of Porous Scaffolds from Chitosan-Collagen-Gelatin Composite. *React. Funct. Polym.* **2016**, *103*, 131−140.
(57) Abdal-Hay, A.; Pant, H. R.; Lim, J. K. Super-Hydrophilic Electrospun Nylon-6/Hydroxyapatite Membrane for Bone Tissue Engineering. *Eur. Polym. J.* **2013**, *49*, 1314−1321.
(58) Shakiba, M.; Ghomi, E. R.; Khosravi, F.; Jouybar, S.; Bigham, A.; Zare, M.; Abdouss, M.; Moaref, R.; Ramakrishna, S. Nylon—A Material Introduction and Overview for Biomedical Applications. *Polym. Adv. Technol.* **2021**, *32*, 3368−3383.
(59) Winnacker, M.; Beringer, A. J.; Gronauer, T. F.; Güngör, H. H.; Reinschlüssel, L.; Rieger, B.; Sieber, S. A. Polyamide/PEG Blends as Biocompatible Biomaterials for the Convenient Regulation of Cell Adhesion and Growth. *Macromol. Rapid Commun.* **2019**, *40*, No. 1900091.
(60) Roldan, L. G.; Kaufman, H. S. Crystallization of Nylon 6. *J. Polym. Sci., Part B: Polym. Lett.* **1963**, *1*, 603−608.
(61) Wojtecki, R. J.; Meador, M. A.; Rowan, S. J. Using the Dynamic Bond to Access Macroscopically Responsive Structurally Dynamic Polymers. *Nat. Mater.* **2010**, *10*, 14−27.
(62) Leja, K.; Lewandowicz, G. Polymer Biodegradation and Biodegradable Polymers - A Review. *Pol. J. Environ. Stud.* **2010**, *19*, 255−266.
(63) Shelah, O.; Wertheimer, S.; Haj-Ali, R.; Lesman, A. Coral-Derived Collagen Fibers for Engineering Aligned Tissues. *Tissue Eng., Part A* **2021**, *27*, 187−200.
(64) Rose, J. B.; Pacelli, S.; El Haj, A. J.; Dua, H. S.; Hopkinson, A.; White, L. J.; Rose, F. R. A. J. Gelatin-Based Materials in Ocular Tissue Engineering. *Materials* **2014**, *7*, 3106−3135.
(65) Niu, X.; Qin, M.; Xu, M.; Zhao, L.; Wei, Y.; Hu, Y.; Lian, X.; Chen, S.; Chen, W.; Huang, D. Coated Electrospun Polyamide-6/Chitosan Scaffold with Hydroxyapatite for Bone Tissue Engineering. *Biomed. Mater.* **2021**, *16*, No. 025014.
(66) Zhuravleva, M.; Gilazieva, Z.; Grigoriev, T. E.; Shepelev, A. D.; Tenchurin, T.; Kamyshinsky, R.; Krasheninnikov, S. V.; Orlov, S.; Caralogli, G.; Archipova, S.; Holterman, M. J.; Mavlikeev, M.; Deev, R. V.; Chvalun, S. N.; Macchiarini, P. In Vitro Assessment of Electrospun Polyamide-6 Scaffolds for Esophageal Tissue Engineering. *J. Biomed. Mater. Res.* **2019**, *107*, 253−268.
(67) Aldana, A. A.; Abraham, G. A. Current Advances in Electrospun Gelatin-Based Scaffolds for Tissue Engineering Applications. *Int. J. Pharm.* **2017**, *523*, 441−453.
(68) Ali, M. G.; Mousa, H. M.; Blaudez, F.; Abd El-sadek, M. S.; Mohamed, M. A.; Abdel-Jaber, G. T.; Abdal-hay, A.; Ivanovski, S. Dual Nanofiber Scaffolds Composed of Polyurethane- Gelatin/Nylon 6-Gelatin for Bone Tissue Engineering. *Colloids Surf., A* **2020**, *597*, No. 124817.
(69) Panthi, G.; Barakat, N. A. M.; Risal, P.; Yousef, A.; Pant, B.; Unnithan, A. R.; Kim, H. Y. Preparation and Characterization of Nylon-6/Gelatin Composite Nanofibers via Electrospinning for Biomedical Applications. *Fibers Polym.* **2013**, *14*, 718−723.
(70) Koosha, K.; Habibi, S.; Talebian, A. Microstructural Study of Nylon-6/Gelatin Composite Nanofibers. *Russ. J. Appl. Chem.* **2017**, *90*, 1640−1647.
(71) Franchi, M.; Trirè, A.; Quaranta, M.; Orsini, E.; Ottani, V. Collagen Structure of Tendon Relates to Function. *Sci. World J.* **2007**, *7*, 404−420.
(72) Bancelin, S.; Lynch, B.; Bonod-Bidaud, C.; Ducourthial, G.; Psilodimitrakopoulos, S.; Dokládal, P.; Allain, J. M.; Schanne-Klein, M. C.; Ruggiero, F. Ex Vivo Multiscale Quantitation of Skin Biomechanics in Wild-Type and Genetically-Modified Mice Using Multiphoton Microscopy. *Sci. Rep.* **2015**, *5*, No. 17635.
(73) Franchi, M.; De Pasquale, V.; Martini, D.; Quaranta, M.; Macciocca, M.; Dionisi, A.; Ottani, V. Contribution of Glycosaminoglycans to the Microstructural Integrity of Fibrillar and Fiber Crimps in Tendons and Ligaments. *Sci. World J.* **2010**, *10*, 1932−1940.
(74) Evans, A. G. Perspective on the Development of High-Toughness Ceramics. *J. Am. Ceram. Soc.* **1990**, *73*, 187−206.
(75) Launey, M. E.; Ritchie, R. O. On the Fracture Toughness of Advanced Materials. *Adv. Mater.* **2009**, *21*, 2103−2110.
(76) Yao, Y.; Allardyce, B. J.; Rajkhowa, R.; Hegh, D.; Qin, S.; Usman, K. A. S.; Mota-Santiago, P.; Zhang, J.; Lynch, P.; Wang, X.; Kaplan, D. L.; Razal, J. M. Toughening Wet-Spun Silk Fibers by Silk Nanofiber Templating. *Macromol. Rapid Commun.* **2022**, *43*, No. 2100891.
(77) Kai, D.; Prabhakaran, M. P.; Stahl, B.; Eblenkamp, M.; Wintermantel, E.; Ramakrishna, S. Mechanical Properties and in Vitro Behavior of Nanofiberhydrogel Composites for Tissue Engineering Applications. *Nanotechnology* **2012**, *23*, No. 095705.
(78) Neves, M. I.; Ara, M.; Moroni, L.; Silva, R. M. P.; Barrias, C. C. The Development of Bioactive Hydrogel Networks. *Molecules* **2020**, *25*, 978.
(79) Ushiki, T. Collagen Fibers, Reticular Fibers and Elastic Fibers. A Comprehensive Understanding from a Morphological Viewpoint. *Arch. Histol. Cytol.* **2002**, *65*, 109−126.
(80) Chow, M. J.; Turcotte, R.; Lin, C. P.; Zhang, Y. Arterial Extracellular Matrix: A Mechanobiological Study of the Contributions and Interactions of Elastin and Collagen. *Biophys. J.* **2014**, *106*, 2684−2692.
(81) Guan, Q.-F.; Bin; Ling, Z. C.; Yin, C. H.; Yu, S. H.; et al. Sustainable Multiscale High-Haze Transparent Cellulose Fiber Film via a Biomimetic Approach. *ACS Mater. Lett.* **2022**, *4*, 87−92.
(82) Guan, Q. F.; Yang, H.; Han, Z. M.; Zhou, L. C.; Zhu, Y. B.; Ling, Z. C.; Jiang, H.; Wang, P. F.; Ma, T.; Wu, H. A.; Yu, S. H. Lightweight, Tough, and Sustainable Cellulose Nanofiber-Derived Bulk Structural Materials with Low Thermal Expansion Coefficient. *Sci. Adv.* **2020**, *6*, No. eaaz1114.
(83) Sugita, S.; Matsumoto, T. Multiphoton Microscopy Observations of 3D Elastin and Collagen Fiber Microstructure Changes during Pressurization in Aortic Media. *Biomech. Model. Mechanobiol.* **2017**, *16*, 763−773.
(84) Amabili, M.; Asgari, M.; Breslavsky, I. D.; Franchini, G.; Giovanniello, F.; Holzapfel, G. A. Microstructural and Mechanical Characterization of the Layers of Human Descending Thoracic Aortas. *Acta Biomater.* **2021**, *134*, 401−421.
(85) Slack, J. M. W.Principles of Tissue Engineering. In *Molecular Biology of the Cell*; Academic Press, 2013.
(86) Mecham, R. P. *The Extracellular Matrix: An Overview*; Elsevier B.V., 2018; Vol. *143*.

https://doi.org/10.1021/acsapm.3c00057
ACS Appl. Polym. Mater. 2023, 5, 2816−2829

(87) Jun, I.; Han, H. S.; Edwards, J. R.; Jeon, H. Electrospun Fibrous Scaffolds for Tissue Engineering: Viewpoints on Architecture and Fabrication. *Int. J. Mol. Sci.* **2018**, *19*, 745.
(88) Li, X.; You, R.; Luo, Z.; Chen, G.; Li, M. Silk Fibroin Scaffolds with a Micro-/Nano-Fibrous Architecture for Dermal Regeneration. *J. Mater. Chem. B* **2016**, *4*, 2903−2912.

https://doi.org/10.1021/acsapm.3c00057
ACS Appl. Polym. Mater. 2023, 5, 2816−2829